The successful incorporation of Ag into single grain, Y–Ba–Cu–O bulk superconductors

The successful incorporation of Ag into single grain, Y–Ba–Cu–O bulk superconductors

Jasmin V J Congreve[1], Yunhua Shi, Anthony R Dennis, John H Durrell and David A Cardwell

Department of Engineering, University of Cambridge, Cambridge, CB2 1PZ, United Kingdom

E-mail: jvjc2@cam.ac.uk

CrossMark

Abstract

The use of RE-Ba–Cu–O [(RE)BCO] bulk superconductors, where RE = Y, Gd, Sm, in practical applications is, at least in part, limited by their mechanical properties and brittle nature, in particular. Alloying these materials with silver, however, produces a significant improvement in strength without any detrimental impact on their superconducting properties. Unfortunately, the top seeded melt growth technique, used routinely to process bulk (RE)BCO superconductors in the form of large, single grains required for practical applications, is complex and has a large number of inter-related variables, so the addition of silver increases the complexity of the growth process even further. This can make successful growth of this system extremely challenging. Here we report measurements of the growth rate of YBCO-Ag fabricated using a new growth technique consisting of continuous cooling and isothermal hold process. The resulting data form the basis of a model that has been used to derive suitable heating profiles for the successful single grain growth of YBCO-Ag bulk superconductors of up to 26 mm in diameter. The microstructure and distribution of silver within these samples have been studied in detail. The maximum trapped field at the top surface of the bulk YBCO-Ag samples has been found to be comparable to that of standard YBCO processed without Ag. The YBCO-Ag samples also exhibit a much more uniform trapped field profile compared to that of YBCO.

Keywords: YBCO, bulk superconductor, TSMG, trapped field, superconductor, YBCO-Ag, single grain

(Some figures may appear in colour only in the online journal)

1. Introduction

Single grain RE-Ba–Cu–O [(RE)BCO] bulk high temperature superconductors, where RE = Y, Gd or Sm, are able to trap large magnetic fields that are significantly larger than those generated by permanent magnets [1, 2]. This means that these materials may find practical application in a wide range of technologies, such as Maglev trains, energy storage systems, rotating electrical machines and trapped flux devices [3–5]. However, the inherently brittle nature of these ceramic-like materials means their mechanical properties can limit the achievable superconducting properties and, hence, their suitability for applications that involve relatively high magnetic forces [6, 7]. The addition of silver to (RE)BCO has been shown to increase both the fracture toughness [8] and the bending strength [9, 10] of the samples without degrading their superconducting properties, unlike many other alloying elements that have been investigated previously [11–13].

Practical applications of bulk superconductors require materials to be processed in the form of large, single grains. The presence of poorly connected, high angle grain boundaries in the

[1] Author to whom any correspondence should be addressed.

(RE)BCO microstructure reduces the flow of supercurrent significantly, which, in turn, reduces the size of the current loop and therefore the magnitude of the trapped field that can be generated by bulk samples [14–17]. Top seeded melt growth (TSMG) is one of the simplest and most widely used methods of fabricating large, single grain bulk YBCO. TSMG involves heating and holding the precursor powder pellet above the peritectic decomposition temperature of the superconducting $YBa_2Cu_3O_{7-\delta}$ (Y-123) phase, whereby it decomposes into a secondary, non-superconducting Y_2BaCuO_5 (Y-211) solid phase and a residual Ba–Cu–O liquid phase. Slow, controlled undercooling in the presence of a suitable seed crystal subsequently enables the nucleation and growth of a large, single grain composed of a continuous superconducting Y-123 matrix but containing a distribution of discrete, non-superconducting Y-211 phase inclusions [14, 18].

The TSMG process is one of the simplest processes for fabricating bulk (RE)BCO materials, although it is based necessarily on the optimization of many associated, inter-dependent variables. Consequently, although the addition of silver improves the mechanical properties of the bulk super-conductor, it concomitantly increases the difficulty of fabrication. The fabrication of large, single grain bulk samples by batch processing has been achieved successfully to date for Y–Ba–Cu–O (YBCO), Gd–Ba–Cu–O–Ag (GdBCO-Ag) and Sm–Ba–Cu–O–Ag (SmBCO-Ag) systems [19], but is much more difficult to achieve for YBCO-Ag. The addition of an excess of 5 wt% Ag to the precursor composition causes a reduction in the peritectic temperature [20] of approximately 30 °C for this material [21], which narrows significantly the temperature window available for successful, single grain growth. The reduction in the maximum processing temperature has many effects on the growth process, including on the decomposition [21], solute diffusion and interface kinetics and, therefore, causes an overall reduction in the growth rate [20]. In addition, there is an increase in the likelihood of the spontaneous nucleation of secondary grains due to the reduction in processing temperature, and further difficulties are associated with the low solubility of silver within the melt in the peritectically decomposed state [22]. Yttrium diffuses much more slowly to the growth front than gadolinium or samarium during solidification in the TSMG process. Further reductions in the diffusion rate due to the lower processing temperature reduces the growth rate yet further, which makes the fabrication of YBCO-Ag much more difficult than that of YBCO, GdBCO-Ag and SmBCO-Ag. This also highlights the requirement for a very different heating profile for the successful growth of YBCO-Ag compared to the YBCO, GdBCO-Ag and SmBCO-Ag systems.

The provision of additional liquid phase material to recycled (RE)BCO samples, in general, and to YBCO samples processed without silver grown in the so-called liquid-phase enriched TSMG process has enabled much more reliable fabrication of large, single YBCO grains. The additional liquid provides a sufficient concentration of the RE element at the growth front, enabling an improved tolerance to the presence of Ce and Ag-rich clusters that typically form during the melt process [23]. For this reason, liquid-phase enriched
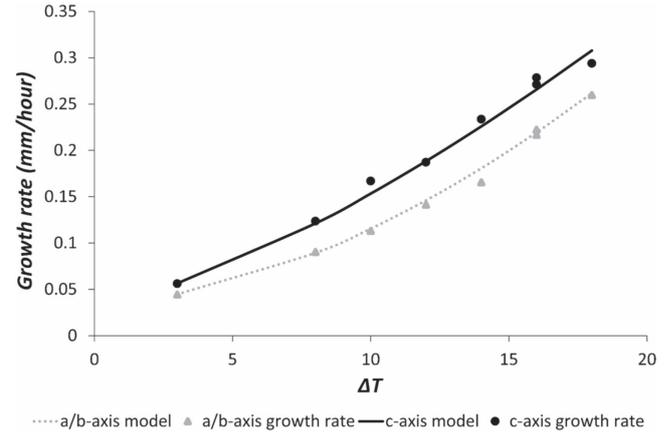

Figure 1. Growth rate in both the a/b- and c-axis directions for partially grown YBCO-Ag samples (indicated by the points) and the growth rate model (shown by the continuous lines) [25].
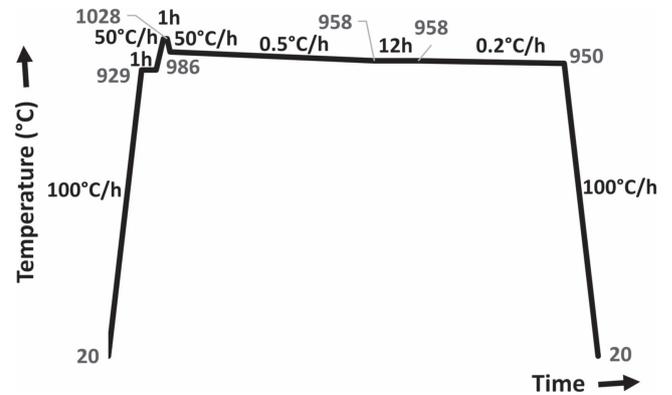

Figure 2. The heating profile used to successfully grow YBCO-Ag samples of 30 mm as-pressed diameter.

TSMG has been used to assist the reliable, successful fabrication of large single grains of YBCO-Ag that have otherwise been difficult to fabricate by conventional TSMG.

A number of studies have been carried out on the growth rate of YBCO fabricated without silver [2, 24], and relationships have been established between growth rate and undercooling. Experimental results are generally in good agreement with these relationships [24]. We recently reported detailed growth rate data for the YBCO-Ag system [25] and a new, two-stage method for the study of growth rate of the YBCO-Ag system; the so-called continuous cooling and isothermal hold (CCIH) technique. The new growth rate model for the YBCO-Ag system described by the following equations and is illustrated alongside the growth rate data from partially grown samples fabricated using the CCIH technique in figure 1:

$$R_{a/b} = 1.4 \times 10^{-3}(\Delta T)^{1.76} + 0.035,$$

$$R_c = 4.5 \times 10^{-3}(\Delta T)^{1.42} + 0.035,$$

where $R_{a/b}$ is growth rate in the a/b-axis direction in mm h^{-1}, R_c is growth rate in the c-axis direction in mm h^{-1} and ΔT is the undercooling below 970 °C [25].
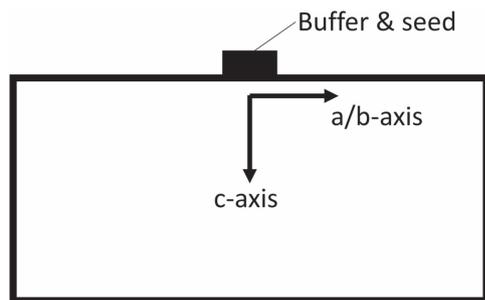
Figure 3. Schematic illustration of the *a/b*- and *c*-axis directions within the bulk, single grain YBCO samples.

Figure 4. YBCO-Ag single grains of diameter (top row) 17 mm, 21 mm (middle row) and 26 mm (bottom row).
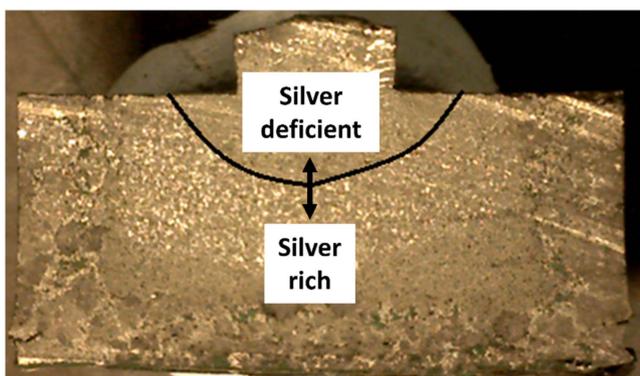

Figure 5. A photograph of the sample undercooled by 18 °C, illustrating the silver-deficient and silver-rich in appearance regions (this microstructure is typical of all the Ag-containing samples fabricated in this study) [25].

The maximum growth rate for the YBCO-Ag system is approximately $0.3\,\mathrm{mm\,h^{-1}}$, which is significantly lower than the maximum growth rate of the YBCO system of $0.6\,\mathrm{mm\,h^{-1}}$ [2, 24]. The significant reduction in growth rate when YBCO is alloyed with silver is one of the major limitations to the ease with which large single grains can be grown successfully. This reduction in growth rate also necessitates a significant change in the heating profile used for successful large grain growth. The growth rate model has been used to derive suitable heating profiles for the successful growth of single grains of samples of YBCO-Ag of various sizes.

Liquid-phase enriched TSMG has been used in the present work to enable the successful fabrication of single grains of YBCO-Ag. The growth rate model derived for the YBCO-Ag system has subsequently enabled a suitable heating profile to be defined for the successful growth of YBCO-Ag single grains of diameter up to 26 mm. The trapped field at the top and bottom of YBCO single grains grown with and without silver addition was measured as part of this study. In addition, the microstructure and composition along both the *a/b*- and *c*-axis of the single grains were observed and trends in the distribution of the silver agglomerates and the Y-211 and Y-123 phases parallel to the sample *c*-axis observed. Conclusions have been drawn on the effect of the addition of silver to YBCO on the microstructure and the superconducting properties of the resulting large, single grains.

2. Method

Fifteen samples were prepared in this study by liquid-phase enriched TSMG [14, 26, 27]. Precursor powder was mixed from 99.9% purity powders of Y-123:Y-211:CeO$_2$:Ag$_2$O in a weight ratio of 150:50:1:20 in order to introduce in excess of 10 wt% Ag$_2$O to the sample. Liquid-phase-rich powder was mixed from Yb$_2$O$_3$:Ba$_3$Cu$_5$O$_8$:BaO$_2$ in the ratio 5.0:5.6:1.0 and then calcined once at 850 °C for 5 h.

Composite green pellets consisting of a layer of liquid-rich powder of varying weight (1.5, 3.2 and 4.6 g) below a layer of precursor powder, also of varying weight (10, 20 and 45 g) were pressed uniaxially in cylindrical dies of diameters 20, 25 and 30 mm. A paste formed from Yb$_2$O$_3$ and ethanol was painted onto the bottom of each pressed pellet to prevent the formation of sub-grains during processing at the base of the sample. This pellet was placed, in turn, onto an array of ZrO$_2$ rods mounted on a ceramic plate. A cylindrical, uni-axially pressed buffer pellet [28–32] of mass 0.15 g and diameter 5 mm composed of Ag-free YBCO was placed at the centre of the top of the precursor pellet. Finally, a generic seed [33] was placed at the centre of the upper surface of the buffer pellet.

The samples were heated in a box furnace to above the peritectic temperature, which was determined by differential thermal analysis to be 989 °C for the precursor containing 10 wt% Ag$_2$O, and held at this temperature for over 1 h to ensure complete peritectic decomposition. The partially molten samples were then cooled rapidly to 970 °C, then more slowly at $0.5\,°\mathrm{C\,h^{-1}}$, held at a constant temperature and then cooled slowly at $0.2\,°\mathrm{C\,h^{-1}}$ to enable controlled grain growth to occur. The extent of the initial slow cooling period was varied in proportion to the diameter of the bulk sample. This, in turn, led to a different undercooling temperatures being attained during the isothermal hold periods. The isothermal holding
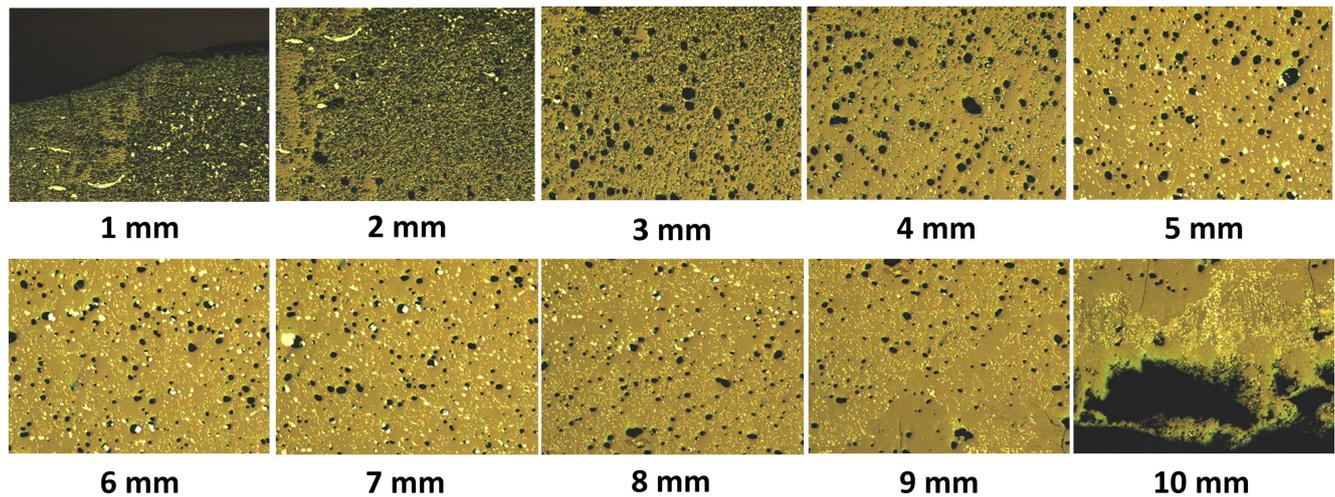
Figure 6. Optical microscope images taken along the *c*-axis direction from directly below the seed for the sample shown in figure 5. The images shown for 1 and 2 mm are within the buffer pellet, and those at 3 and 4 mm are within the silver-deficient region.
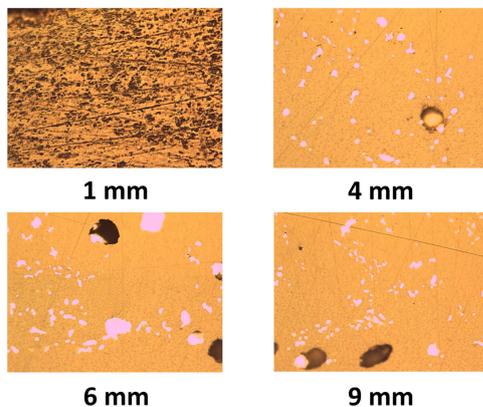

Figure 7. Images of the sample shown in figure 5 at 500× magnification. The silver distribution (white regions), Y-211 inclusions (dark grey small regions), Y-123 matrix and the pore distribution (black) can be seen clearly.

time was also derived from the growth rate; the total slow cooling and isothermal hold time was determined by the growth rate model from the calculated time taken for the single grain to extend radially to the edge of the sample and vertically to its base. The heating profile used for growth of a 30 mm as-pressed diameter sample is shown in figure 2.

The cross sections of a number of the partially grown samples derived from the growth rate study [25] were polished using silicon carbide paper followed by diamond paste. The samples were imaged using an optical microscope. A magnification of 50× was used to observe the pore and crack distribution, while magnification of 1000× was used to observe the size and distribution of the embedded Y-211 inclusions. Images were taken at 1 mm intervals from the top of the buffer pellet in the *c*-axis direction and in the *a/b*-axis direction at approximately 1.5 mm vertically from the top of the sample. The *a/b* and *c*-axes of the single grain sample are illustrated schematically in figure 3.

The microstructures of the samples were also observed within areas of approximately 40 µm × 40 µm along the two axes at 1 mm intervals using a scanning electron microscope at

2000× magnification with an acceleration voltage of 25 kV. The average composition for each of the areas imaged was recorded using an energy dispersive x-ray spectroscopy analyser (s-3400). Normalization of the composition data in atomic percent with respect to Y, Ba and Cu and Y, Ba, Cu and Ag present at each location was carried out, and the variation in each set of the normalized composition data was observed. The ratios of Y:Ba and Y:Cu were calculated, and found to correlate directly with the amount of Y-211 present at the relevant part of the sample. As a result, these data can be used to observe the trend in the Y-211 distribution throughout the samples.

A number of the fully grown samples of as-pressed diameter 20, 25 and 30 mm were annealed in an oxygen-rich environment for 8 d. The excess liquid-rich layer was removed from the base of the oxygenated samples and the top and bottom surfaces were polished flat and parallel. The samples were field cooled in an applied field of 1.4 T. The maximum trapped field at the top and bottom surfaces was measured at 77 K using a hand-held Hall sensor at a distance of 0.5 mm above the respective surface. The trapped field profiles of both the top and bottom surfaces were measured using a rotating array of 20 Hall probes positioned 1 ± 0.5 mm above the surface of each sample.

3. Results

Six 17 mm, five 21 mm and four 26 mm diameter samples were grown successfully as part of this study, as shown in figure 4. The requirement for the slow cooling period, in addition to the isothermal hold period is evident from the structure of the bulk samples. The cross-section of each of the samples shows the same general trend in silver distribution. The region directly below the buffer appears to be silver deficient compared to the central region. The silver agglomerates in the 'silver-deficient' region are much smaller in size than those in the central silver-rich region, as evident from figure 5. Silver is forced to the growth front during the initial stages of growth, since it cannot be incorporated easily into
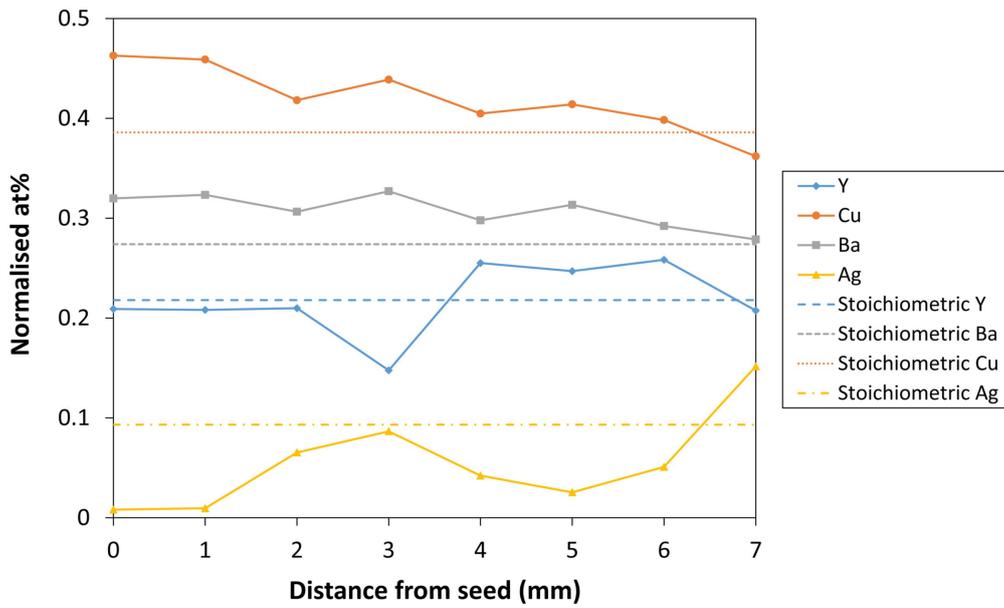
Figure 8. Composition within the sample undercooled at 18 °C. The distribution of silver is as expected from the other images.
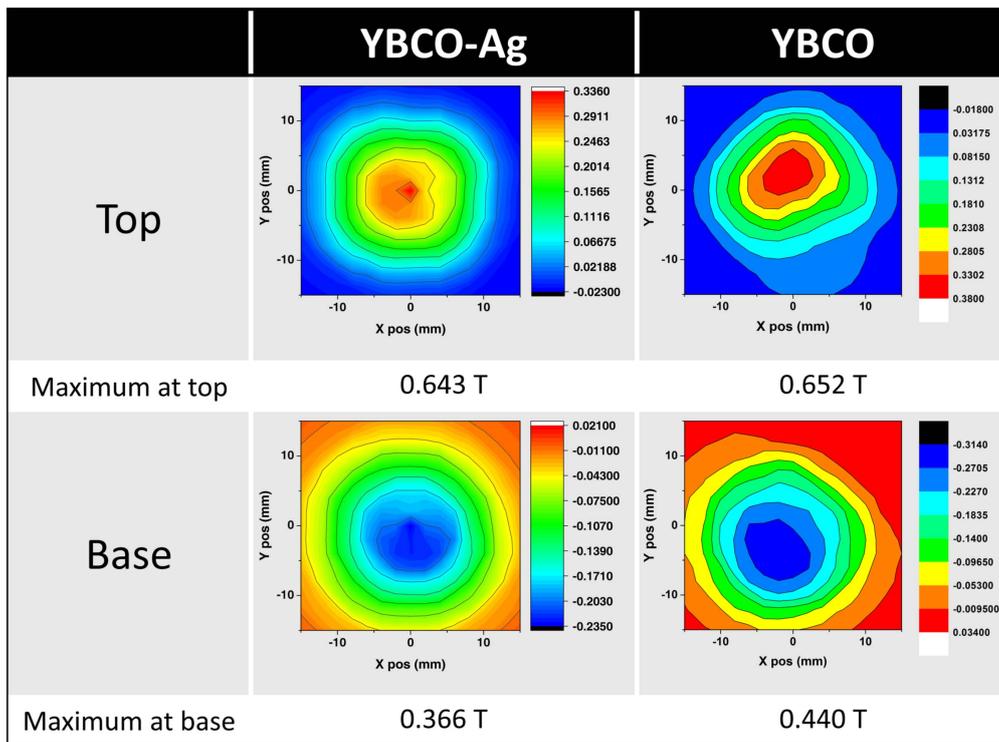

Figure 9. Trapped field profiles of YBCO-Ag and YBCO of 26 mm diameter. The maximum values are comparable and the trapped field profile is much more uniform for YBCO-Ag.

Table 1. Average maximum trapped field at the top and base for the samples of 17, 21 and 26 mm samples of YBCO-Ag.

Sample diameter (mm)	Maximum trapped field (T)	
	Top	Base
17	0.36 ± 0.11	0.25 ± 0.09
21	0.39 ± 0.04	0.30 ± 0.03
26	0.56 ± 0.08	0.32 ± 0.09

the Y-123 lattice. The excess of silver is ultimately too great for it to be pushed by the growth front as it advances, and is, therefore, forced into the pores already present within the solidifying single grain structure. This produces a discontinuity where a transition from a silver-deficient region to a silver-rich region occurs. The silver agglomerates are much larger from this point onwards, and fill some of the regions that were initially pores.

Observations of the microstructure were carried out for a number of the partially grown, non-oxygenated samples at both 50× and 1000× magnification using an optical microscope. These were made both along the *a/b*-axis direction at the top of the sample and along the *c*-axis direction. The distinction between the single-grain region and the region outside of the single grain is clearly visible in these samples. The average pore size within the single grain region is much smaller with fewer pores and many more large silver agglomerates, which suggests that a greater number of pores are filled by silver agglomerates within this region. Figure 6 shows optical microscope images of an almost fully grown sample before oxygenation, held at an undercooling of 18 °C for 45 min, which illustrates more clearly the distribution of silver agglomerates in the sample microstructure. The images taken at 2 and 3 mm from the top surface of the sample correspond to the region within the buffer pellet, which contains a large number of small pores and a limited number of small silver agglomerates. The images at 3 and 4 mm lie within the region that appears to be silver deficient in figure 5. It can be seen from these images that there are silver agglomerates present in this region, an example of which is labelled in the figure. However, the silver agglomerates in the 'silver-deficient' appearing region are much smaller in size and there are many fewer silver agglomerates in this region compared to the region that appears to be silver rich.

Figure 7 shows images taken at a much higher magnification of 500×. These were used to observe the silver distribution within the bulk microstructure more closely and enable the distribution of Y-211 agglomerates to be observed. The image taken at 2 mm from the top is within the buffer pellet, where many small pores (black) are present within the Y-123 matrix and there are no visible silver agglomerates. The image taken at 4 mm along the *c*-axis direction, which lies in the 'silver-deficient' region labelled in figure 6, contains one relatively large pore (very dark grey), a small number of very small pores (black), a number of small silver agglomerates (white) and a uniform distribution of Y-211 particles (pale grey) within the Y-123 matrix. Much larger silver agglomerates are present with increasing distance from the seed in the 'silver-rich' region and more, larger pores are also present. This suggests that the silver initially fills pores that are present within the bulk prior to any diffusion that occurs during the growth process. Many of the large pores are filled by the additional liquid towards the base of the sample, where fewer pores are available initially to be filled by silver agglomerates, and hence there are smaller and fewer silver agglomerates in this region of the sample.

The composition of the partially grown samples observed using the optical microscope was analysed at intervals of 1 mm along the same axes, as shown in figure 8. A sudden transition can be seen in the normalized at% of Y at the edge of the single grain region. The data in figure 8 are for the same sample shown in figure 5, which is almost fully grown. The observed normalized at% of silver is as expected from the microscope images; at the top of the sample the at% of silver is low, but increases with distance in the 'silver-rich' region. More of the pores are filled as the distance from the seed increases further towards the region containing additional liquid, and the presence of silver agglomerates is less evident, and those that are present are much smaller in size.

The maximum trapped field at the top surface of a randomly chosen YBCO-Ag sample of diameter 26 mm was measured to be 0.643 T, which is comparable with that of a randomly chosen YBCO sample grown by liquid-phase enriched TSMG (0.652 T), as shown in figure 9. The trapped field profiles show that both samples were successfully grown in the form of a single grain and the more circular and parallel lines in the trapped field profile of the YBCO-Ag sample shows that the trapped field distribution is much more uniform in this sample than in the standard YBCO sample. The maximum trapped field of the other samples were measured and are summarized in table 1.

4. Conclusions

The growth rate model for the YBCO-Ag system has enabled suitable heating profiles to be derived to successfully grow large single grains of YBCO-Ag. We are now able to reliably and successfully grow large single grains of YBCO-Ag that exhibit more uniform and consistent trapped field properties than YBCO single grains of the same size processed without silver with comparable magnitude maximum surface trapped field. We have seen that the distribution of silver is not uniform throughout the cross-section of the bulk microstructure due to the fundamental nature of the growth process. It is difficult to incorporate the silver into the YBCO lattice during the initial stages of growth. In consequence, silver is pushed by the growth front, generating a silver deficient region below the seed that contains only a limited concentration of small silver agglomerates. Once the level of silver at the growth front reaches a threshold, however, silver is incorporated into the bulk microstructure to yield a discontinuity in the silver distribution. Many more and much larger silver agglomerates are present further away from the seed and fill regions that were initially pores. The filling of pores by the silver agglomerates reduces the porosity and therefore is likely to improve the strength of the initially brittle YBCO bulk material, which is important for practical applications of these technologically important materials.

Acknowledgments

ORCID iDs

Jasmin V J Congreve ⬤ https://orcid.org/0000-0002-2025-2155
John H Durrell ⬤ https://orcid.org/0000-0003-0712-3102

References

[1] Durrell J H et al 2014 A trapped field of 17.6T in melt-processed, bulk Gd–Ba–Cu–O reinforced with shrink-fit steel Supercond. Sci. Technol. **27** 082001

[2] Zhai W, Shi Y H, Durrell J H, Dennis A R and Cardwell D A 2014 The influence of Y-211 content on the growth rate and Y-211 distribution in Y–Ba–Cu–O single grains fabricated by top seeded melt growth Cryst. Growth Des. **14** 6367–75

[3] Campbell A M and Cardwell D A 1997 Bulk high temperature superconductors for magnet applications Cryogenics **37** 567–75

[4] Werfel F N, Floegel-Delor U, Rothfeld R, Riedel T, Goebel B, Wippich D and Schirrmeister P 2012 Superconductor bearings, flywheels and transportation Supercond. Sci. Technol. **25** 014007

[5] Li B Z, Zhou D F, Xu K, Hara S, Tsuzuki K, Miki M, Felder B, Deng Z G and Izumi M 2012 Materials process and applications of single grain (RE)-Ba–Cu–O bulk high-temperature superconductors Physica C **482** 50–7

[6] Nishio T, Itoh Y, Ogasawara F, Suganuma M, Yamada Y and Mizutani U 1989 Superconducting and mechanical-properties of YBCO-Ag composite superconductors J. Mater. Sci. **24** 3228–34

[7] Iida K, Babu N H, Shi Y H, Miyazaki T, Sakai N, Murakami M and Cardwell D A 2008 Single domain YBCO/Ag bulk superconductors fabricated by seeded infiltration and growth J. Phys.: Conf. Ser. **97** 012105

[8] Diko P, Krabbes G and Wende C 2001 Influence of Ag addition on crystallization and microstructure of melt-grown single-grain $YBa_2Cu_3O_7$ bulk superconductors Supercond. Sci. Technol. **14** 486–95

[9] Nakamura Y, Tachibana K and Fujimoto H 1998 Dispersion of silver in the melt grown $YBa_2Cu_3O_{6+x}$ crystal Physica C **306** 259–70

[10] Yeh F and White K W 1991 Fracture-toughness behavior of the $YBa_2Cu_3O_{7-x}$ superconducting ceramic with silver-oxide additions J. Appl. Phys. **70** 4989–94

[11] Azambuja P d, Rodrigues P Jr, Jurelo A R, Serbena F C, Foerster C E, Costa R M, Souza G B d, Lepienski C M and Chinelatto A L 2009 Effects of Ag addition on some physical properties of granular $YBa_2Cu_3O_{7-\delta}$ superconductor Braz. J. Phys. **39** 638–44

[12] Mendoza E, Puig T, Varesi E, Carrillo A E, Plain J and Obradors X 2000 Critical current enhancement in YBCO-Ag melt-textured composites: influence of microcrack density Physica C **334** 7–14

[13] Matsui M, Sakai N and Murakami M 2002 Effect of Ag_2O addition on the trapped fields and mechanical properties of Nd–Ba–Cu–O bulk superconductors Supercond. Sci. Technol. **15** 1092

[14] Cardwell D A 1998 Processing and properties of large grain (RE)BCO Mater. Sci. Eng. B **53** 1–10

[15] Dimos D, Chaudhari P, Mannhart J and Legoues F K 1988 Orientation dependence of grain-boundary critical currents in $YBa_2Cu_3O_{7-\delta}$ bicrystals Phys. Rev. Lett. **61** 219–22

[16] Todt V R, Zhang X F, Miller D J, St Louis Weber M and Dravid V P 1996 Controlled growth of bulk bicrystals and the investigation of microstructure-property relations of $YBa_2Cu_3O_x$ grain boundaries Appl. Phys. Lett. **69** 3746–8

[17] Durrell J H, Hogg M J, Kahlmann F, Barber Z H, Blamire M G and Evetts J E 2003 Critical current of $YBa_2Cu_3O_{7-\delta}$ low-angle grain boundaries Phys. Rev. Lett. **90** 247006

[18] Fujimoto H, Murakami M, Gotoh S, Koshizuka N, Oyama T, Shiohara Y and Tanaka S 1990 Melt processing of YBaCuO oxide superconductors Advances in Superconductivity II: Proc. of the 2nd Int. Symp. on Superconductivity pp 285–8

[19] Shi Y, Babu N H, Iida K, Yeoh W K, Dennis A R, Pathak S K and Cardwell D A 2010 Batch-processed GdBCO-Ag bulk superconductors fabricated using generic seeds with high trapped fields Physica C **470** 685–8

[20] Iida K, Babu N H, Shi Y, Miyazaki T and Sakai N 2008 Single domain YBCO/Ag bulk superconductors fabricated by seeded infiltration and growth J. Phys.: Conf. Ser. **97** 012105

[21] Cai C, Tachibana K and Fujimoto H 2000 Study on single-domain growth of $Y_{1.8}Ba_{2.4}Cu_{3.4}O_y$/Ag system by using Nd123/MgO thin film as seed Supercond. Sci. Technol. **13** 698

[22] Reddy E S, Goodilin E A, Tarka M, Zeisberger M and Schmitz G J 2002 Low temperature processing of single domain $YBa_2Cu_3O_y$ thick films from Y_2O_3 fabrics on Ag–Pd alloy substrates Physica C **372–376** 1200–3

[23] Shi Y, Namburi D K, Wang M, Durrell J, Dennis A and Cardwell D 2015 A reliable method for recycling (Sm, Gd, Y)$Ba_2Cu_3O_{7-\delta}$ bulk superconductors J. Am. Ceram. Soc. **98** 2760

[24] Endo A, Chauhan H S, Nakamura Y and Shiohara Y 1996 Relationship between growth rate and undercooling in Pt-added $Y_1Ba_2Cu_3O_{7-x}$ J. Mater. Res. **11** 1114–9

[25] Congreve J V J, Shi Y, Dennis A R, Durrell J H and Cardwell D A 2017 The successful incorporation of Ag into single grain, Y–Ba–Cu–O bulk superconductors IOP Conf. Ser.: Mater. Sci. Eng. **279** 012027

[26] Congreve J V J, Shi Y H, Dennis A R, Durrell J H and Cardwell D A 2017 Improvements in the processing of large grain, bulk Y–Ba–Cu–O superconductors via the use of additional liquid phase Supercond. Sci. Technol. **30** 11

[27] Li G Z, Li D J, Deng X Y, Deng J H and Yang W M 2013 Infiltration growth and crystallization characterization of single-grain Y–Ba–Cu–O bulk superconductors Cryst. Growth Des. **13** 1246–51

[28] Li T Y, Cheng L, Yan S B, Sun L J, Yao X, Yoshida Y and Ikuta H 2010 Growth and superconductivity of REBCO bulk processed by a seed/buffer layer/precursor construction Supercond. Sci. Technol. **23** 125002

[29] Kim C J, Lee J H, Park S D, Jun B H, Han S C and Han Y H 2011 Y_2BaCuO_5 buffer block as a diffusion barrier for samarium in top seeded melt growth processed $YBa_2Cu_3O_{7-y}$ superconductors using a $SmBa_2Cu_3O_{7-d}$ seed Supercond. Sci. Technol. **24** 015008

[30] Zhou D F, Xu K, Hara S, Li B Z, Deng Z G, Tsuzuki K and Izumi M 2012 MgO buffer-layer-induced texture growth of RE-Ba–Cu–O bulk Supercond. Sci. Technol. **25** 025022

[31] Shi Y H, Dennis A R and Cardwell D A 2015 A new seeding technique for the reliable fabrication of large, SmBCO single grains containing silver using top seeded melt growth Supercond. Sci. Technol. **28** 035014

[32] Kumar N D, Shi Y H, Zhai W, Dennis A R, Durrell J H and Cardwell D A 2015 Buffer pellets for high-yield, top-seeded melt growth of large grain Y–Ba–Cu–O superconductors Cryst. Growth Des. **15** 1472–80

[33] Shi Y, Babu N H and Cardwell D A 2005 Development of a generic seed crystal for the fabrication of large grain (RE)-Ba–Cu–O bulk superconductors Supercond. Sci. Technol. **18** L13–6